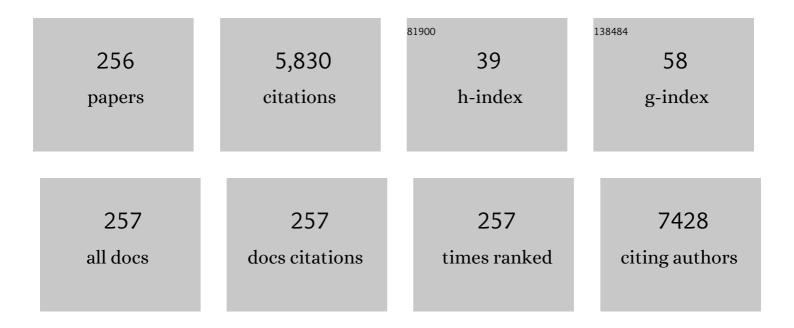
Byong-Taek Lee

List of Publications by Year in descending order

Source: https://exaly.com/author-pdf/1950978/publications.pdf Version: 2024-02-01



#	Article	IF	CITATIONS
1	Physical and in-vitro biological evaluations of plant based nano cellulose loaded injectable bone substitutes. Materials Technology, 2022, 37, 1742-1754.	3.0	2
2	Fabrication of thrombin loaded TEMPO-oxidized cellulose nanofiber-gelatin sponges and their hemostatic behavior in rat liver hemorrhage model. Journal of Biomaterials Science, Polymer Edition, 2022, 33, 499-516.	3.5	9
3	Autologous stromal vascular fraction-loaded hyaluronic acid/gelatin-biphasic calcium phosphate scaffold for bone tissue regeneration. Materials Science and Engineering C, 2022, 132, 112533.	7.3	12
4	Porous <scp>CDHA</scp> microspheres laden brushiteâ€based injectable bone substitutes for improved bone regeneration. Journal of Biomedical Materials Research - Part B Applied Biomaterials, 2022, , .	3.4	1
5	Development of a novel polycaprolactone based composite membrane for periodontal regeneration using spin coating technique. Journal of Biomaterials Science, Polymer Edition, 2022, 33, 783-800.	3.5	11
6	Physico-mechanical and biological evaluation of heparin/VEGF-loaded electrospun polycaprolactone/decellularized rat aorta extracellular matrix for small-diameter vascular grafts. Journal of Biomaterials Science, Polymer Edition, 2022, 33, 1664-1684.	3.5	9
7	Tailored alginate/PCL-gelatin-β-TCP membrane for guided bone regeneration. Biomedical Materials (Bristol), 2022, 17, 045011.	3.3	6
8	In-vitro and in-vivo biocompatibility of dECM-alginate as a promising candidate in cell delivery for kidney regeneration. International Journal of Biological Macromolecules, 2022, 211, 616-625.	7.5	13
9	Small-diameter decellularized vascular graft with electrospun polycaprolactone. Materials Letters, 2021, 284, 128973.	2.6	11
10	Synthesis and characterization of biphasic calcium phosphate laden thiolated hyaluronic acid hydrogel based scaffold: physical and <i>in-vitro</i> biocompatibility evaluations. Journal of Biomaterials Science, Polymer Edition, 2021, 32, 337-354.	3.5	5
11	Fibroblast cell derived extracellular matrix containing electrospun scaffold as a hybrid biomaterial to promote in vitro endothelial cell expansion and functionalization. Materials Science and Engineering C, 2021, 120, 111659.	7.3	11
12	Boosting osteogenic potential and bone regeneration by co-cultured cell derived extracellular matrix incorporated porous electrospun scaffold. Journal of Biomaterials Science, Polymer Edition, 2021, 32, 779-798.	3.5	7
13	<i>In Vivo</i> Comparison of Three Human Acellular Dermal Matrices for Breast Reconstruction. In Vivo, 2021, 35, 2719-2728.	1.3	5
14	An Impact of Different Silicone Breast Implants on the Bacterial Attachment and Growth. Journal of Biomaterials and Nanobiotechnology, 2021, 12, 21-33.	0.5	2
15	Physico-mechanical and biological evaluation of an injectable m-TG cross-linked thrombin loaded amended gelatin hemostat to heal liver trauma. International Journal of Biological Macromolecules, 2021, 181, 339-348.	7.5	7
16	Early-stage bone regeneration of hyaluronic acid supplemented with porous 45s5 bioglass-derived granules: an injectable system. Biomedical Materials (Bristol), 2021, 16, 045034.	3.3	4
17	Polycaprolactone-gelatin membrane as a sealant biomaterial efficiently prevents postoperative anastomotic leakage with promoting tissue repair. Journal of Biomaterials Science, Polymer Edition, 2021, 32, 1530-1547.	3.5	9
18	Silicone Implants Immobilized with Interleukin-4 Promote the M2 Polarization of Macrophages and Inhibit the Formation of Fibrous Capsules. Polymers, 2021, 13, 2630.	4.5	6

#	Article	IF	CITATIONS
19	Functionalization of Silicone Surface with Drugs and Polymers for Regulation of Capsular Contracture. Polymers, 2021, 13, 2731.	4.5	4
20	Multi-functional nanocellulose-chitosan dressing loaded with antibacterial lawsone for rapid hemostasis and cutaneous wound healing. Carbohydrate Polymers, 2021, 272, 118482.	10.2	56
21	In-vitro and in-vivo hemostat evaluation of decellularized liver extra cellular matrix loaded chitosan/gelatin spongy scaffolds for liver injury. International Journal of Biological Macromolecules, 2021, 193, 638-646.	7.5	11
22	Fabrication of injectable bone substitute loading porous simvastatin-loaded poly(lactic- <i>co</i> -glycolic acid) microspheres. International Journal of Polymeric Materials and Polymeric Biomaterials, 2020, 69, 351-362.	3.4	1
23	Collagen and bone morphogenetic proteinâ€2 functionalized hydroxyapatite scaffolds induce osteogenic differentiation in human adiposeâ€derived stem cells. Journal of Biomedical Materials Research - Part B Applied Biomaterials, 2020, 108, 1363-1371.	3.4	14
24	A biphasic calcium phosphate ceramic scaffold loaded with oxidized cellulose nanofiber–gelatin hydrogel with immobilized simvastatin drug for osteogenic differentiation. Journal of Biomedical Materials Research - Part B Applied Biomaterials, 2020, 108, 1229-1238.	3.4	9
25	Controlled release of Mitomycin C from modified cellulose based thermo-gel prevents post-operative de novo peritoneal adhesion. Carbohydrate Polymers, 2020, 229, 115552.	10.2	26
26	Preliminary studies on the in vivo performance of various kinds of nanocellulose for biomedical applications. Journal of Biomaterials Applications, 2020, 34, 942-951.	2.4	17
27	Curcumin incorporation into an oxidized cellulose nanofiber-polyvinyl alcohol hydrogel system promotes wound healing. Materials and Design, 2020, 186, 108313.	7.0	106
28	Soya protein isolate-polyethylene oxide electrospun nanofiber membrane with bone marrow-derived mesenchymal stem cell for enhanced bone regeneration. Journal of Biomaterials Applications, 2020, 34, 1142-1149.	2.4	6
29	Local support among arctic residents to a land tenure reform in Finnmark, Norway. Land Use Policy, 2020, 91, 104326.	5.6	2
30	Novel TOCNF reinforced injectable alginate / \hat{l}^2 -tricalcium phosphate microspheres for bone regeneration. Materials and Design, 2020, 194, 108892.	7.0	23
31	Functionalization of extracellular matrix (ECM) on multichannel biphasic calcium phosphate (BCP) granules for improved bone regeneration. Materials and Design, 2020, 192, 108653.	7.0	7
32	Mechanically and Electrically Enhanced Polyurethane-poly(3,4-ethylenedioxythiophene) Conductive Foams with Aligned Pore Structures Promote MC3T3-E1 Cell Growth and Proliferation. ACS Applied Polymer Materials, 2020, 2, 1482-1490.	4.4	5
33	In vitro endothelial differentiation evaluation on polycaprolactone-methoxy polyethylene glycol electrospun membrane and fabrication of multilayered small-diameter hybrid vascular graft. Journal of Biomaterials Applications, 2020, 34, 1395-1408.	2.4	14
34	In vitro and in vivo evaluation of Ca/P-hyaluronic acid/gelatin based novel dental plugs for one-step socket preservation. Materials and Design, 2020, 194, 108891.	7.0	27
35	Thermal stimuli-responsive hyaluronic acid loaded cellulose based physical hydrogel for post-surgical de novo peritoneal adhesion prevention. Materials Science and Engineering C, 2020, 110, 110661.	7.3	23
36	Comparative study on biodegradation and biocompatibility of multichannel calcium phosphate based bone substitutes. Materials Science and Engineering C, 2020, 110, 110694.	7.3	22

#	Article	IF	CITATIONS
37	Evaluation of bone regeneration potential of injectable extracellular matrix (ECM) from porcine dermis loaded with biphasic calcium phosphate (BCP) powder. Materials Science and Engineering C, 2020, 110, 110663.	7.3	25
38	Thermal cycling effect on osteogenic differentiation of MC3T3-E1 cells loaded on 3D-porous Biphasic Calcium Phosphate (BCP) scaffolds for early osteogenesis. Materials Science and Engineering C, 2019, 105, 110027.	7.3	24
39	Preparation and evaluation of BCP SDâ€agarose composite microsphere for bone tissue engineering. Journal of Biomedical Materials Research - Part B Applied Biomaterials, 2019, 107, 2263-2272.	3.4	17
40	Enhanced decellularization technique of porcine dermal ECM for tissue engineering applications. Materials Science and Engineering C, 2019, 104, 109841.	7.3	56
41	In vitro and in vivo evaluation of bioglass microspheres incorporated brushite cement for bone regeneration. Materials Science and Engineering C, 2019, 103, 109775.	7.3	35
42	TEMPO oxidized nano-cellulose containing thermo-responsive injectable hydrogel for post-surgical peritoneal tissue adhesion prevention. Materials Science and Engineering C, 2019, 102, 12-21.	7.3	43
43	Bone regeneration of multichannel biphasic calcium phosphate granules supplemented with hyaluronic acid. Materials Science and Engineering C, 2019, 99, 1058-1066.	7.3	25
44	Enhancement of hemostatic property of plant derived oxidized nanocellulose-silk fibroin based scaffolds by thrombin loading. Carbohydrate Polymers, 2019, 208, 168-179.	10.2	44
45	Investigation of efficiency of a novel, zinc oxide loaded TEMPO-oxidized cellulose nanofiber based hemostat for topical bleeding. International Journal of Biological Macromolecules, 2019, 126, 786-795.	7.5	38
46	Hemostasis and Bone Regeneration Using Chitosan/Gelatin-BCP Bi-layer Composite Material. ASAIO Journal, 2019, 65, 620-627.	1.6	11
47	Incorporation of chitosan-alginate complex into injectable calcium phosphate cement system as a bone graft material. Materials Science and Engineering C, 2019, 94, 385-392.	7.3	50
48	Bone regeneration strategy by different sized multichanneled biphasic calcium phosphate granules: In vivo evaluation in rabbit model. Journal of Biomaterials Applications, 2018, 32, 1406-1420.	2.4	12
49	Multi-channel biphasic calcium phosphate granules as cell carrier capable of supporting osteogenic priming of mesenchymal stem cells. Materials and Design, 2018, 141, 142-149.	7.0	8
50	Fabrication of an electroconductive, flexible, and soft poly(3,4-ethylenedioxythiophene)–thermoplastic polyurethane hybrid scaffold by <i>in situ</i> vapor phase polymerization. Journal of Materials Chemistry B, 2018, 6, 4082-4088.	5.8	16
51	Comparative Bone Regeneration Potential Studies of Collagen, Heparin, and Polydopamine-Coated Multichannelled BCP Granules. ASAIO Journal, 2018, 64, 115-121.	1.6	4
52	Functionalization of porous BCP scaffold by generating cellâ€derived extracellular matrix from rat bone marrow stem cells culture for bone tissue engineering. Journal of Tissue Engineering and Regenerative Medicine, 2018, 12, e1256-e1267.	2.7	32
53	In vitro and in vivo acute response towards injectable thermosensitive chitosan/TEMPO-oxidized cellulose nanofiber hydrogel. Carbohydrate Polymers, 2018, 180, 246-255.	10.2	66
54	Streamlined System for Conducting <i>In Vitro</i> Studies Using Decellularized Kidney Scaffolds. Tissue Engineering - Part C: Methods, 2018, 24, 42-55.	2.1	7

#	Article	IF	CITATIONS
55	Effects of plateletâ€rich plasma on biological activity and bone regeneration of brushiteâ€based calcium phosphate cement. Journal of Biomedical Materials Research - Part B Applied Biomaterials, 2018, 106, 2316-2326.	3.4	7
56	A novel hybrid multichannel biphasic calcium phosphate granule-based composite scaffold for cartilage tissue regeneration. Journal of Biomaterials Applications, 2018, 32, 775-787.	2.4	19
57	Development and properties of duplex MgF2/PCL coatings on biodegradable magnesium alloy for biomedical applications. PLoS ONE, 2018, 13, e0193927.	2.5	25
58	In-vitro and in-vivo evaluation of hemostatic potential of decellularized ECM hydrogels. Materials Letters, 2018, 232, 130-133.	2.6	9
59	Development of fibrous balloon for facilitating the use of calcium phosphate cement in vertebral augmentation procedures. Materials and Design, 2018, 158, 172-183.	7.0	4
60	<i>In vitro</i> and <i>in vivo</i> assessment of biomedical Mg–Ca alloys for bone implant applications. Journal of Applied Biomaterials and Functional Materials, 2018, 16, 126-136.	1.6	47
61	<i>In vivo</i> evaluation of injectable calcium phosphate cement composed of Zn―and Si―incorporated βâ€tricalcium phosphate and monocalcium phosphate monohydrate for a critical sized defect of the rabbit femoral condyle. Journal of Biomedical Materials Research - Part B Applied Biomaterials, 2017, 105, 260-271.	3.4	24
62	Phosphonate-chitosan functionalization of a multi-channel hydroxyapatite scaffold for interfacial implant-bone tissue integration. Journal of Materials Chemistry B, 2017, 5, 1293-1301.	5.8	17
63	Enzymatic <i>in situ</i> formed hydrogel from gelatin–tyramine and chitosan-4-hydroxylphenyl acetamide for the co-delivery of human adipose-derived stem cells and platelet-derived growth factor towards vascularization. Biomedical Materials (Bristol), 2017, 12, 015026.	3.3	20
64	Bone morphogenetic proteinâ€2 immobilization on porous PCLâ€BCPâ€Col composite scaffolds for bone tissue engineering. Journal of Applied Polymer Science, 2017, 134, 45186.	2.6	18
65	Development of BMP-2 immobilized polydopamine mediated multichannelled biphasic calcium phosphate granules for improved bone regeneration. Materials Letters, 2017, 208, 122-125.	2.6	12
66	Plant-derived oxidized nanofibrillar cellulose-chitosan composite as an absorbable hemostat. Materials Letters, 2017, 197, 150-155.	2.6	28
67	Incorporation of BMP-2 loaded collagen conjugated BCP granules in calcium phosphate cement based injectable bone substitutes for improved bone regeneration. Materials Science and Engineering C, 2017, 77, 713-724.	7.3	39
68	Preparation and characterization of polycaprolactone–polyethylene glycol methyl ether and polycaprolactone–chitosan electrospun mats potential for vascular tissue engineering. Journal of Biomaterials Applications, 2017, 32, 648-662.	2.4	36
69	A hybrid composite system of biphasic calcium phosphate granules loaded with hyaluronic acid–gelatin hydrogel for bone regeneration. Journal of Biomaterials Applications, 2017, 32, 433-445.	2.4	39
70	In vitro and in vivo evaluation of effectiveness of a novel TEMPO-oxidized cellulose nanofiber-silk fibroin scaffold in wound healing. Carbohydrate Polymers, 2017, 177, 284-296.	10.2	96
71	In vitro biocompatibility of vapour phase polymerised conductive scaffolds for cell lines. Polymer, 2017, 124, 95-100.	3.8	24
72	Cryptotanshinone promotes commitment to the brown adipocyte lineage and mitochondrial biogenesis in C3H10T1/2 mesenchymal stem cells via AMPK and p38-MAPK signaling. Biochimica Et Biophysica Acta - Molecular and Cell Biology of Lipids, 2017, 1862, 1110-1120.	2.4	44

#	Article	IF	CITATIONS
73	Examination of In vitro and In vivo biocompatibility of alginate-hyaluronic acid microbeads As a promising method in cell delivery for kidney regeneration. International Journal of Biological Macromolecules, 2017, 105, 143-153.	7.5	30
74	Evaluation of egg white ovomucin-based porous scaffold as an implantable biomaterial for tissue engineering. , 2017, 105, 2107-2117.		23
75	Augmenting inÂvitro osteogenesis of a glycine–arginine–glycine–aspartic-conjugated oxidized alginate–gelatin–biphasic calcium phosphate hydrogel composite and inÂvivo bone biogenesis through stem cell delivery. Journal of Biomaterials Applications, 2016, 31, 661-673.	2.4	6
76	Designing of Combined Nano and Microfiber Network by Immobilization of Oxidized Cellulose Nanofiber on Polycaprolactone Fibrous Scaffold. Journal of Biomedical Nanotechnology, 2016, 12, 1864-1875.	1.1	29
77	Collagen-hydroxyapatite coated unprocessed cuttlefish bone as a bone substitute. Materials Letters, 2016, 181, 156-160.	2.6	13
78	Brushite-based calcium phosphate cement with multichannel hydroxyapatite granule loading for improved bone regeneration. Journal of Biomaterials Applications, 2016, 30, 823-837.	2.4	18
79	A Study of BMP-2-Loaded Bipotential Electrolytic Complex around a Biphasic Calcium Phosphate-Derived (BCP) Scaffold for Repair of Large Segmental Bone Defect. PLoS ONE, 2016, 11, e0163708.	2.5	11
80	Hard tissue regeneration using bone substitutes: an update on innovations in materials. Korean Journal of Internal Medicine, 2015, 30, 279.	1.7	61
81	Osteogenic potential of simvastatin loaded gelatin-nanofibrillar cellulose-β tricalcium phosphate hydrogel scaffold in critical-sized rat calvarial defect. European Polymer Journal, 2015, 73, 308-323.	5.4	27
82	Nanoparticle Biphasic Calcium Phosphate Loading on Gelatin-Pectin Scaffold for Improved Bone Regeneration. Tissue Engineering - Part A, 2015, 21, 1376-1387.	3.1	33
83	Collagen immobilization of multi-layered BCP-ZrO 2 bone substitutes to enhance bone formation. Applied Surface Science, 2015, 345, 238-248.	6.1	10
84	Bone formation of a porous Gelatin-Pectin-biphasic calcium phosphate composite in presence of BMP-2 and VEGF. International Journal of Biological Macromolecules, 2015, 76, 10-24.	7.5	67
85	Effect of rat bone marrow derived–stem cell delivery from serum-loaded oxidized alginate–gelatin–biphasic calcium phosphate hydrogel for bone tissue regeneration using a nude mouse critical-sized calvarial defect model. Journal of Bioactive and Compatible Polymers, 2015, 30, 188-208.	2.1	9
86	Preformed chitosan cryogel-biphasic calcium phosphate: a potential injectable biocomposite for pathologic fracture. Journal of Biomaterials Applications, 2015, 30, 182-192.	2.4	19
87	Effect of Local Sustainable Release of BMP2-VEGF from Nano-Cellulose Loaded in Sponge Biphasic Calcium Phosphate on Bone Regeneration. Tissue Engineering - Part A, 2015, 21, 1822-1836.	3.1	67
88	Improved In Vitro Biocompatibility of Surface-Modified Hydroxyapatite Sponge Scaffold with Gelatin and BMP-2 in Comparison Against a Commercial Bone Allograft. ASAIO Journal, 2015, 61, 78-86.	1.6	8
89	Bilayer electrospun poly(vinyl alcohol)–gelatin mat and biphasic calcium phosphate–pectin–gelatin hydrogel for application in bone hemorrhage. Journal of Bioactive and Compatible Polymers, 2015, 30, 424-435.	2.1	2
90	HAp granules encapsulated oxidized alginate–gelatin–biphasic calcium phosphate hydrogel for bone regeneration. International Journal of Biological Macromolecules, 2015, 81, 898-911.	7.5	43

#	Article	IF	CITATIONS
91	Bone Regeneration Using Hydroxyapatite Sponge Scaffolds with In Vivo Deposited Extracellular Matrix. Tissue Engineering - Part A, 2015, 21, 2649-2661.	3.1	18
92	The effect of BMPâ€2 and VEGF loading of gelatinâ€pectinâ€BCP scaffolds to enhance osteoblast proliferation. Journal of Applied Polymer Science, 2015, 132, .	2.6	19
93	Chitosan–hyaluronic acid polyelectrolyte complex scaffold crosslinked with genipin for immobilization and controlled release of BMP-2. Carbohydrate Polymers, 2015, 115, 160-169.	10.2	130
94	Platelet-rich plasma encapsulation in hyaluronic acid/gelatin-BCP hydrogel for growth factor delivery in BCP sponge scaffold for bone regeneration. Journal of Biomaterials Applications, 2015, 29, 988-1002.	2.4	39
95	The effects of dimethyl 3,3′-dithiobispropionimidate di-hydrochloride cross-linking of collagen and gelatin coating on porous spherical biphasic calcium phosphate granules. Journal of Biomaterials Applications, 2014, 29, 386-398.	2.4	3
96	Synthesis of a novel bioactive glass using the ultrasonic energy assisted hydrothermal method and their biocompatibility evaluation. Journal of Materials Research, 2014, 29, 1781-1789.	2.6	4
97	Evaluation of the cytocompatibility hemocompatibility <i>in vivo</i> bone tissue regenerating capability of different PCL blends. Journal of Biomaterials Science, Polymer Edition, 2014, 25, 487-503.	3.5	39
98	A Combination of Biphasic Calcium Phosphate Scaffold with Hyaluronic Acid-Gelatin Hydrogel as a New Tool for Bone Regeneration. Tissue Engineering - Part A, 2014, 20, 1993-2004.	3.1	83
99	Evaluation of the potential antiâ€adhesion effect of the PVA/Gelatin membrane. Journal of Biomedical Materials Research - Part B Applied Biomaterials, 2014, 102, 840-849.	3.4	46
100	Surface modification of porous polycaprolactone/biphasic calcium phosphate scaffolds for bone regeneration in rat calvaria defect. Journal of Biomaterials Applications, 2014, 29, 624-635.	2.4	9
101	Utilization of PVPA and its effect on the material properties and biocompatibility of PVA electrospun membrane. Polymers for Advanced Technologies, 2014, 25, 55-65.	3.2	15
102	Fabrication of recombinant human bone morphogenetic protein-2 coated porous biphasic calcium phosphate-sodium carboxymethylcellulose-gelatin scaffold and its In vitro evaluation. Macromolecular Research, 2014, 22, 1297-1305.	2.4	7
103	In Vitro Study of CaTiO3–Hydroxyapatite Composites for Bone Tissue Engineering. ASAIO Journal, 2014, 60, 722-729.	1.6	15
104	Fabrication of Porous Hydroxyapatite Scaffolds as Artificial Bone Preform and its Biocompatibility Evaluation. ASAIO Journal, 2014, 60, 216-223.	1.6	36
105	Poly(vinylphosphonic acid) immobilized on chitosan: A glycosaminoglycan-inspired matrix for bone regeneration. International Journal of Biological Macromolecules, 2014, 64, 294-301.	7.5	20
106	Biphasic calcium phosphate loading on polycaprolactone/poly(lacto- <i>co</i> -glycolic acid) membranes for improved tensile strength, inÂvitro biocompatibility, and inÂvivo tissue regeneration. Journal of Biomaterials Applications, 2014, 28, 1164-1179.	2.4	6
107	<i>In vitro</i> and <i>in vivo</i> evaluation of porous PCL-PLLA 3D polymer scaffolds fabricated via salt leaching method for bone tissue engineering applications. Journal of Biomaterials Science, Polymer Edition, 2014, 25, 150-167.	3.5	45
108	Bioactive glass incorporation in calcium phosphate cement-based injectable bone substitute for improved <i>inÂvitro</i> biocompatibility and <i>inÂvivo</i> bone regeneration. Journal of Biomaterials Applications, 2014, 28, 739-756.	2.4	49

#	Article	IF	CITATIONS
109	<i>In Vitro</i> and <i>In Vivo</i> Studies of BMP-2-Loaded PCL–Gelatin–BCP Electrospun Scaffolds. Tissue Engineering - Part A, 2014, 20, 3279-3289.	3.1	62
110	BMP-2 Immoblized in BCP-Chitosan-Hyaluronic Acid Hybrid Scaffold for Bone Tissue Engineering. Korean Journal of Materials Research, 2014, 24, 704~709-704~709.	0.2	3
111	Electrospun PLGA/gelatin fibrous tubes for the application of biodegradable intestinal stent in rat model. Journal of Biomedical Materials Research - Part B Applied Biomaterials, 2013, 101B, 1095-1105.	3.4	30
112	A hybrid electrospun PU/PCL scaffold satisfied the requirements of blood vessel prosthesis in terms of mechanical properties, pore size, and biocompatibility. Journal of Biomaterials Science, Polymer Edition, 2013, 24, 1692-1706.	3.5	41
113	Fabrication and in vitro evaluations with osteoblast-like MG-63 cells of porous hyaluronic acid-gelatin blend scaffold for bone tissue engineering applications. Journal of Materials Science, 2013, 48, 4233-4242.	3.7	19
114	Bio-functionalization of polycaprolactone infiltrated BCP scaffold with silicon and fibronectin enhances osteoblast activity in vitro. Applied Surface Science, 2013, 279, 13-22.	6.1	10
115	Fabrication and biocompatibility of novel bilayer scaffold for skin tissue engineering applications. Journal of Biomaterials Applications, 2013, 27, 605-615.	2.4	59
116	Fabrication and characterization of ZrO2–CaO–P2O5–Na2O–SiO2 bioactive glass ceramics. Journal of Materials Science, 2013, 48, 1863-1872.	3.7	24
117	Functional nanofiber mat of polyvinyl alcohol/gelatin containing nanoparticles of biphasic calcium phosphate for bone regeneration in rat calvaria defects. Journal of Biomedical Materials Research - Part A, 2013, 101A, 2412-2423.	4.0	54
118	Microstructure and biocompatibility of composite biomaterials fabricated from titanium and tricalcium phosphate by spark plasma sintering. Journal of Biomedical Materials Research - Part A, 2013, 101A, 1489-1501.	4.0	23
119	Preparation and characterization of PLGA microspheres by the electrospraying method for delivering simvastatin for bone regeneration. International Journal of Pharmaceutics, 2013, 443, 87-94.	5.2	122
120	Hybrid hydroxyapatite nanoparticles-loaded PCL/GE blend fibers for bone tissue engineering. Journal of Biomaterials Science, Polymer Edition, 2013, 24, 520-538.	3.5	45
121	Poly(lactide-co-glycolide acid)/biphasic calcium phosphate composite coating on a porous scaffold to deliver simvastatin for bone tissue engineering. Journal of Drug Targeting, 2013, 21, 719-729.	4.4	14
122	<i>In vitro</i> and <i>in vivo</i> studies of rhBMP2 oated PS/PCL fibrous scaffolds for bone regeneration. Journal of Biomedical Materials Research - Part A, 2013, 101A, 797-808.	4.0	26
123	<i>In vitro</i> and <i>in vivo</i> evaluation of electrospun PCL/PMMA fibrous scaffolds for bone regeneration. Science and Technology of Advanced Materials, 2013, 14, 015009.	6.1	75
124	Fabrication of multilayer ZrO ₂ –biphasic calcium phosphate–poly-caprolactone unidirectional channeled scaffold for bone tissue formation. Journal of Biomaterials Applications, 2013, 28, 462-472.	2.4	15
125	A novel fibrous scaffold composed of electrospun porous poly(É›-caprolactone) fibers for bone tissue engineering. Journal of Biomaterials Applications, 2013, 28, 514-528.	2.4	23
126	Addition of Hydroxyapatite to Toothpaste and Its Effect to Dentin Remineralization. Korean Journal of Materials Research, 2013, 23, 168-176.	0.2	5

#	Article	IF	CITATIONS
127	Residual Stress on Concentric Laminated Fibrous Al2O3-ZrO2Composites on Prolonged High Temperature Exposure. Korean Journal of Materials Research, 2013, 23, 531-536.	0.2	Ο
128	On Stabilization of PVPA/PVA Electrospun Nanofiber Membrane and Its Effect on Material Properties and Biocompatibility. Journal of Nanomaterials, 2012, 2012, 1-9.	2.7	34
129	Microwave sintering and <i>in vitro</i> study of defect-free stable porous multilayered HAp–ZrO ₂ artificial bone scaffold. Science and Technology of Advanced Materials, 2012, 13, 035009.	6.1	16
130	The effect of cross-linking on the microstructure, mechanical properties and biocompatibility of electrospun polycaprolactone–gelatin/PLGA–gelatin/PLGA–chitosan hybrid composite. Science and Technology of Advanced Materials, 2012, 13, 035002.	6.1	48
131	Fabrication and material properties of fibrous PHBV scaffolds depending on the cross-ply angle for tissue engineering. Journal of Biomaterials Applications, 2012, 27, 457-468.	2.4	2
132	Evaluation of formation process of spherical porous biphasic calcium phosphate (BCP) granules by slurry dripping method. Metals and Materials International, 2012, 18, 717-721.	3.4	3
133	Electrospinning of polyvinyl alcohol/gelatin nanofiber composites and cross-linking for bone tissue engineering application. Journal of Biomaterials Applications, 2012, 27, 255-266.	2.4	102
134	Fabrication of oxidized alginate-gelatin-BCP hydrogels and evaluation of the microstructure, material properties and biocompatibility for bone tissue regeneration. Journal of Biomaterials Applications, 2012, 27, 311-321.	2.4	80
135	Fabrication of novel multilayer Al2O3–(m-ZrO2)/t-ZrO2 fibrous ceramics composites. Ceramics International, 2012, 38, 1043-1050.	4.8	2
136	Preparation and characterization of a novel 3D scaffold from poly(É›-caprolactone)/biphasic calcium phosphate hybrid composite microspheres adhesion. Biochemical Engineering Journal, 2012, 64, 76-83.	3.6	23
137	Formation of TiO2 nano fibers on a micro-channeled Al2O3–ZrO2/TiO2 porous composite membrane for photocatalytic filtration. Journal of the European Ceramic Society, 2012, 32, 657-663.	5.7	23
138	Novel approach to the fabrication of an artificial small bone using a combination of sponge replica and electrospinning methods. Science and Technology of Advanced Materials, 2011, 12, 035002.	6.1	20
139	In Vitro and In Vivo Evaluations of 3D Porous TCP-coated and Non-coated Alumina Scaffolds. Journal of Biomaterials Applications, 2011, 25, 539-558.	2.4	11
140	Comparative Study of Microstructures and Material Properties in the Vacuum and Spark Plasma Sintered Ti-Calcium Phosphate Composites. Materials Transactions, 2011, 52, 1436-1442.	1.2	8
141	A Novel Photoactive Nano-Filtration Module Composed of a TiO ₂ Loaded PVA Nano-Fibrous Membrane on Sponge Al ₂ O ₃ Scaffolds and Al ₂ O ₃ -(m-ZrO ₂)/t-ZrO ₂ Composites. Materials Transactions. 2011, 52, 1452-1456.	1.2	7
142	Enhanced osteoconduction and angiogenesis of a three dimensional continuously porous Al2O3 implant. Materials Science and Engineering C, 2011, 31, 1458-1465.	7.3	4
143	Microstructure control of TCP/TCP-(t-ZrO2)/t-ZrO2 composites for artificial cortical bone. Materials Science and Engineering C, 2011, 31, 1660-1666.	7.3	15
144	Fabrication and characterization of porous poly(lactic-co-glycolic acid) (PLGA) microspheres for use as a drug delivery system. Journal of Materials Science, 2011, 46, 2510-2517.	3.7	23

#	Article	IF	CITATIONS
145	Fabrication of photocatalytic PVA–TiO2 nano-fibrous hybrid membrane using the electro-spinning method. Journal of Materials Science, 2011, 46, 5615-5620.	3.7	47
146	Preparation and characterization of electrospun PCL/PLGA membranes and chitosan/gelatin hydrogels for skin bioengineering applications. Journal of Materials Science: Materials in Medicine, 2011, 22, 2207-2218.	3.6	73
147	Nano Ag loaded PVA nanoâ€fibrous mats for skin applications. Journal of Biomedical Materials Research - Part B Applied Biomaterials, 2011, 96B, 225-233.	3.4	67
148	Preparation and characterization of novel poly(ε aprolactone)/biphasic calcium phosphate hybrid composite microspheres. Journal of Biomedical Materials Research - Part B Applied Biomaterials, 2011, 98B, 272-279.	3.4	13
149	Formation and characterization of porous spherical biphasic calcium phosphate (BCP) granules using PCL. Ceramics International, 2011, 37, 2043-2049.	4.8	11
150	Synthesis of functional gradient BCP/ZrO2 bone substitutes using ZrO2 and BCP nanopowders. Journal of the European Ceramic Society, 2011, 31, 1541-1548.	5.7	32
151	Fabrication of Cross-linked Nano-Fibrous Chitosan Membranes and Their Biocompatibility Evaluation. Korean Journal of Materials Research, 2011, 21, 125-132.	0.2	2
152	Fabrication and Characterization of Strengthened BCP Scaffold Through Infiltration of PCL in the Frame. Bioceramics Development and Applications, 2011, 1, 1-4.	0.3	2
153	Synthesis of Bioactive Glass by Microwave Energy Irradiation and Its In-Vitro Biocompatibility. Bioceramics Development and Applications, 2011, 1, 1-3.	0.3	12
154	Fabrication of Hybrid Composites Consists of Poly Methyl Methacrylate and Polyvinyl Alcohol and Hydroxyapatite. Bioceramics Development and Applications, 2011, 1, 1-4.	0.3	1
155	The Evaluation of Fabrication Parameters Process Effect on the Formation of Poly(lactic-co-glycolic) Tj ETQq1 1).784314 1.9	rgBT /Overlo
156	<i>In vitro</i> and <i>in vivo</i> evaluation of a macro porous β-TCP granule-shaped bone substitute fabricated by the fibrous monolithic process. Biomedical Materials (Bristol), 2010, 5, 035007.	3.3	18
157	Co-Axially Laminated Continuously Porous Composites in Al ₂ 0 ₃ -(m-ZrO ₂)/t-ZrO _{2& System for High Mechanical Strength. Materials Transactions, 2010, 51, 2168-2172.}	lt;/ £ ØB&g	t; 1
158	Fabrication of seven cells in single tubular solid oxide fuel cell using multi-pass extrusion process. Ceramics International, 2010, 36, 1577-1580.	4.8	2
159	Fabrication of β-Si3N4 whiskers from a GPSed-RBSN sponge using 6Y2O3–2MgO additives. Ceramics International, 2010, 36, 2427-2430.	4.8	6
160	Electro-spinning of PLGA/PCL blends for tissue engineering and their biocompatibility. Journal of Materials Science: Materials in Medicine, 2010, 21, 1969-1978.	3.6	151
161	Fabrication of calcium phosphate–calcium sulfate injectable bone substitute using hydroxy-propyl-methyl-cellulose and citric acid. Journal of Materials Science: Materials in Medicine, 2010, 21, 1867-1874.	3.6	35
162	Initial biocompatibility and enhanced osteoblast response of Si doping in a porous BCP bone graft substitute. Journal of Materials Science: Materials in Medicine, 2010, 21, 1937-1947.	3.6	21

#	Article	IF	CITATIONS
163	Fabrication of polyvinyl alcohol/gelatin nanofiber composites and evaluation of their material properties. Journal of Biomedical Materials Research - Part B Applied Biomaterials, 2010, 95B, 184-191.	3.4	108
164	In vitro bioactivity and biocompatibility of calcium phosphate cements using Hydroxy-propyl-methyl-Cellulose (HPMC). Applied Surface Science, 2010, 257, 1533-1539.	6.1	24
165	Fabrication of Ag nanoparticles dispersed in PVA nanowire mats by microwave irradiation and electro-spinning. Materials Science and Engineering C, 2010, 30, 944-950.	7.3	46
166	Evaluation and comparison of the microstructure and mechanical properties of fibrous Al2O3–(m-ZrO2)/t-ZrO2 composites after multiple extrusion steps. Ceramics International, 2010, 36, 1971-1976.	4.8	13
167	<i>In Vitro</i> and <i>In Vivo</i> Evaluation Of Calcium Phosphate Bone Graft Substitutes. Materials Science Forum, 2010, 654-656, 2065-2070.	0.3	0
168	Biomimetic Artificial Cortical Bone with Aligned Microstructure Formed by a Combination of Multi-Extrusion and Rolling Processes. Materials Science Forum, 2010, 654-656, 2237-2240.	0.3	0
169	Fabrication of Artificial Bone by the Combination of Electrospinning, Extrusion and Slurry Processes. Materials Science Forum, 2010, 654-656, 2233-2236.	0.3	0
170	Fabrication and evaluation of powder injection molded Fe–Ni sintered bodies using nano Fe–50%Ni powder. Journal of Alloys and Compounds, 2010, 491, 391-394.	5.5	20
171	Fabrication of Bone Substitutes by the Sponge Replica Method. Materials Science Forum, 2010, 654-656, 2245-2248.	0.3	3
172	PCL Infiltration into a BCP Scaffold Strut to Improve the Mechanical Strength while Retaining Other Properties. Korean Journal of Materials Research, 2010, 20, 331~337-331~337.	0.2	9
173	Fabrication and Characterization of BCP Nano Particle Loaded PCL Fiber and Their Biocompatibility. Korean Journal of Materials Research, 2010, 20, 392-400.	0.2	2
174	Effect of Strontium Doped Porous BCP as Bone Graft Substitutes on Osteoblast. Korean Journal of Materials Research, 2010, 20, 155-160.	0.2	2
175	Biocompatibility of Multilayer Poly Methyl Methacrylate (PMMA)/Poly Vinyl Alcohol (PVA) Bone Plate by Electrospinning Method. Korean Journal of Materials Research, 2010, 20, 312-318.	0.2	1
176	Fabrication and Characterization of Ag-coated BCP Scaffold Derived from Sponge Replica Process. Korean Journal of Materials Research, 2010, 20, 418-422.	0.2	0
177	Fabrication of super-high-strength microchanneled Al2O3–ZrO2 ceramic composites with fibrous microstructure. Scripta Materialia, 2009, 61, 686-689.	5.2	11
178	Fabrication and characterization of porous unidirectional Si2N2O–Si3N4 composite. Materials Letters, 2009, 63, 168-170.	2.6	5
179	Fabrication of platinum coating on continuous porous SiC–Si3N4 composites by the electroless deposition process. Journal of Materials Processing Technology, 2009, 209, 2958-2962.	6.3	3
180	Fabrication of bioglass infiltrated Al2O3–(m-ZrO2) composites. Journal of Materials Science: Materials in Medicine, 2009, 20, 265-269.	3.6	1

#	Article	IF	CITATIONS
181	Fabrication of calcium phosphate-calcium sulfate injectable bone substitute using chitosan and citric acid. Journal of Materials Science: Materials in Medicine, 2009, 20, 935-941.	3.6	35
182	Fabrication and Microstructure Characterization of Continuous Porous TiO ₂ /Al ₂ O ₃ Composite Membrane. Journal of the American Ceramic Society, 2009, 92, 911-915.	3.8	3
183	Formation of rod-like Si3N4 grains in porous SRBSN bodies using 6Y2O3–2MgO sintering additives. Ceramics International, 2009, 35, 2305-2310.	4.8	28
184	Fabrication of fibrous Al2O3-(m-ZrO2)/HAp-(t-ZrO2) core/shell composites with elongated grain formation. Journal of the Ceramic Society of Japan, 2009, 117, 152-156.	1.1	0
185	Fabrication and characterization of t-ZrO2 supported small tubular SOFC. Journal of the Ceramic Society of Japan, 2009, 117, 1131-1133.	1.1	1
186	Fabrication and microstructure characterization of dense and porous SiC-Si3N4/AlN composites using multi-pass extrusion process. Journal of the Ceramic Society of Japan, 2009, 117, 171-174.	1.1	0
187	Fabrication and Characterization of Porous Hydroxyapatite Scaffolds. Korean Journal of Materials Research, 2009, 19, 680-685.	0.2	5
188	Fabrication of biphasic calcium phosphates/polycaprolactone composites by melt infiltration process. Journal of Materials Science: Materials in Medicine, 2008, 19, 2223-2229.	3.6	15
189	Effect of the addition of t-ZrO2 on the material properties of β-TCP/PCL composites. Journal of Materials Science, 2008, 43, 4450-4454.	3.7	3
190	Microstructure and material properties of double-network type fibrous (Al2O3–m-ZrO2)/t-ZrO2 composites. Journal of the European Ceramic Society, 2008, 28, 229-233.	5.7	16
191	Microstructure characterization and electrical conductivity of electroless nano Ni coated 8YSZ cermets. Surface and Coatings Technology, 2008, 202, 2182-2188.	4.8	19
192	Nanosilver-Coated Porous SiC-Si3N4Composite Using Microwave-Assisted Process. Journal of the American Ceramic Society, 2008, 91, 2509-2513.	3.8	5
193	A Novel Method to Fabricate Unidirectional Porous Hydroxyapatite Body Using Ethanol Bubbles in a Viscous Slurry. Journal of the American Ceramic Society, 2008, 91, 3125-3127.	3.8	27
194	Formation of AlN nanowires using Al powder. Materials Chemistry and Physics, 2008, 112, 562-565.	4.0	33
195	Novel Bamboo-Like Fibrous, Micro-Channeled and Functional Gradient Microstructure Control of Ceramics. Materials Transactions, 2008, 49, 339-344.	1.2	3
196	Microstructures and Mechanical Properties of Spark Plasma Sintered Al ₂ O ₃ -Co Composites Using Electroless Deposited Al ₂ O ₃ -Co Powders. Materials Transactions, 2008, 49, 1451-1455.	1.2	3
197	Fabrication and Characterization of Porous TCP coated Al2O3Scaffold by Polymeric Sponge Method. Journal of the Korean Ceramic Society, 2008, 45, 579-583.	2.3	1
198	Effects of Macrophage on Biodegradation of β-tricalcium Phosphate Bone Graft Substitute. Journal of the Korean Ceramic Society, 2008, 45, 618-624.	2.3	3

#	Article	IF	CITATIONS
199	Synthesis of Si2N2O nanowires in porous Si2N2O–Si3N4 substrate using Si powder. Journal of Materials Research, 2007, 22, 615-620.	2.6	11
200	Relationship between microstructure and mechanical properties of fibrous HAp-(t-ZrO2)/Al2O3-(m-ZrO2) composites. Materials Science & Engineering A: Structural Materials: Properties, Microstructure and Processing, 2007, 458, 11-16.	5.6	8
201	Functionally Gradient and Micro-Channeled Al2O3?(t-ZrO2)/HAp Composites. Journal of the American Ceramic Society, 2007, 90, 629-631.	3.8	10
202	Novel Design of Microchanneled Tubular Solid Oxide Fuel Cells and Synthesis Using a Multipass Extrusion Process. Journal of the American Ceramic Society, 2007, 90, 1921-1925.	3.8	11
203	In situ synthesis of spherical BCP nanopowders by microwave assisted process. Materials Chemistry and Physics, 2007, 104, 249-253.	4.0	71
204	Microstructure characterization of fibrous HAp-(20Âvol.% t-ZrO2)/Al2O3-(25Âvol.% m-ZrO2) composites by multi-pass extrusion process. Materials Letters, 2007, 61, 405-408.	2.6	3
205	Fabrication and material properties of powder injection molded Fe sintered bodies using nano Fe powder. Materials Letters, 2007, 61, 1218-1222.	2.6	12
206	Fabrication and microstructure characterization of continuously porous Si2N2O–Si3N4 ceramics. Materials Letters, 2007, 61, 2182-2186.	2.6	18
207	Synthesis and characterization of nano-Ag spot-coated polymethylmethacrylate powders by hydrothermal-assisted attachment method. Materials Letters, 2007, 61, 4177-4180.	2.6	9
208	Microstructure characterization of in situ synthesized porous Si3N4–Si2N2O composites using feldspar additive. Journal of Materials Science, 2007, 42, 4701-4706.	3.7	8
209	Microstructures and material properties of fibrous HAp/Al2O3–ZrO2 composites fabricated by multi-pass extrusion process. Journal of the European Ceramic Society, 2007, 27, 157-163.	5.7	18
210	Fabrication of Porous β-TCP Bone Graft Substitutes Using PMMA Powder and their Biocompatibility Study. Korean Journal of Materials Research, 2007, 17, 318~322-318~322.	0.2	8
211	Fabrication of Porous Al2O3-(m-ZrO2) Composites and Al2O3-(m-ZrO2)/PMMA Hybrid Composites by Infiltration Process. Journal of the Korean Ceramic Society, 2007, 44, 291-296.	2.3	2
212	Effect of MgO-P2O5Sintering Additive on Microstructure of Sintered Hydroxyapatite (HAp) Bodies and Their In-Vitro Study. Korean Journal of Materials Research, 2007, 17, 100-106.	0.2	0
213	In-Situ Fabrication of Micro-channeled Multi Tubular Solid Oxide Fuel Cell using Multi-pass Extrusion Process. Korean Journal of Materials Research, 2007, 17, 313-317.	0.2	0
214	Fabrication of HAp-Coated Micro-Channelled t-ZrO2 Bodies by the Multi-Pass Extrusion Process. Journal of the American Ceramic Society, 2006, 89, 2051-2056.	3.8	5
215	Effect of Addition of Silicon on the Microstructures and Bending Strength of Continuous Porous SiC-Si3N4 Composites. Journal of the American Ceramic Society, 2006, 89, 2057-2062.	3.8	18
216	Microstructure control of continuously porous t-ZrO2 bodies fabricated by multi-pass extrusion process. Materials Science & Engineering A: Structural Materials: Properties, Microstructure and Processing, 2006, 419, 269-275.	5.6	28

#	Article	IF	CITATIONS
217	Microstructures and fracture characteristics of spark plasma-sintered HAp–5vol.% Ag composites. Materials Science & Engineering A: Structural Materials: Properties, Microstructure and Processing, 2006, 429, 348-352.	5.6	22
218	Core/shell volume effect on the microstructure and mechanical properties of fibrous Al2O3–(m-ZrO2)/t-ZrO2 composite. Materials Science & Engineering A: Structural Materials: Properties, Microstructure and Processing, 2006, 432, 317-323.	5.6	10
219	Fabrication of continuously porous SiC–Si3N4 composite using SiC powder by extrusion process. Journal of the European Ceramic Society, 2006, 26, 2467-2473.	5.7	34
220	Fabrication of TiO2–ZrO2 coating on continuously porous SiC–Si3N4 composites. Surface and Coatings Technology, 2006, 201, 519-525.	4.8	4
221	Fabrication of pore-gradient Al2O3–ZrO2 sintered bodies by fibrous monolithic process. Journal of the European Ceramic Society, 2006, 26, 3525-3530.	5.7	26
222	Microstructure and mechanical properties of porous yttria stabilized zirconia ceramic using poly methyl methacrylate powder. Scripta Materialia, 2006, 54, 2081-2085.	5.2	74
223	Synthesis of high purity nano-sized hydroxyapatite powder by microwave-hydrothermal method. Materials Chemistry and Physics, 2006, 99, 235-239.	4.0	189
224	TEM microstructure characterization of nano TiO2 coated on nano ZrO2 powders and their photocatalytic activity. Materials Letters, 2006, 60, 2101-2104.	2.6	20
225	Microstructural characterization of Al2O3–Ni composites prepared by electroless deposition. Surface and Coatings Technology, 2005, 192, 39-42.	4.8	20
226	Pretreatment effect on the synthesis of Ag-coated Al2O3 powders by electroless deposition process. Surface and Coatings Technology, 2005, 195, 333-337.	4.8	27
227	Fabrication of a Continuously Oriented Porous Al ₂ O ₃ Body and Its <i>In Vitro</i> Study. Journal of the American Ceramic Society, 2005, 88, 2262-2266.	3.8	46
228	Relationship Between Microstructures and Material Properties of Novel Fibrous Al2O3-(m-ZrO2)/t-ZrO2 Composites. Journal of the American Ceramic Society, 2005, 88, 2874-2878.	3.8	28
229	Microstructure and osteoblast adhesion of continuously porous Al2O3 body fabricated by fibrous monolithic process. Materials Letters, 2005, 59, 69-73.	2.6	8
230	Microstructure of sol–gel synthesized Al2O3–ZrO2(Y2O3) nano-composites studied by transmission electron microscopy. Materials Letters, 2005, 59, 355-360.	2.6	20
231	Characterization of nano-structured TiN thin films prepared by R.F. magnetron sputtering. Materials Letters, 2005, 59, 3929-3932.	2.6	33
232	Microstructures and bond strengths of plasma-sprayed hydroxyapatite coatings on porous titanium substrates. Journal of Materials Science: Materials in Medicine, 2005, 16, 635-640.	3.6	36
233	Microstructure and Indentation Fracture of Dysprosium Niobate. Journal of Materials Research, 2005, 20, 1422-1427.	2.6	1
234	Microstructures and material properties of fibrous Al2O3–(m-ZrO2)/t-ZrO2 composites fabricated by a fibrous monolithic process. Journal of Materials Research, 2004, 19, 3234-3241.	2.6	34

#	Article	IF	CITATIONS
235	Magneto-electronic properties of Ge1â^'Mn thin films grown by MBE. Journal of Magnetism and Magnetic Materials, 2004, 272-276, E1539-E1540.	2.3	6
236	Anodizing Properties of High Dielectric Oxide Films Coated on Aluminum by Sol-Gel Method. Journal of Electroceramics, 2004, 13, 111-116.	2.0	43
237	Effect of carbon addition on the microstructure of Si 3 N 4 –C fiber composites using semiconductor-waste Si sludge. Journal of the European Ceramic Society, 2004, 24, 2313-2318.	5.7	8
238	Effect of sintering additives on the nitridation behavior of reaction-bonded silicon nitride. Materials Science & Engineering A: Structural Materials: Properties, Microstructure and Processing, 2004, 364, 126-131.	5.6	37
239	Microstructures of porous Al2O3–50 wt.% ZrO2 composites using in-situ synthesized Al2O3–ZrO2 composite powders. Materials Letters, 2004, 58, 2181-2185.	2.6	20
240	Comparison of fracture characteristic of silicon nitride ceramics with and without second crystalline phase. Materials Letters, 2004, 58, 74-79.	2.6	8
241	Microstructure Control of Fiber-like TiN Particles in Hot Pressed Si ₃ N ₄ -O’SiAlON-TiN Composites. Materials Transactions, 2004, 45, 161-164.	1.2	1
242	Microstructure Control of Al ₂ O ₃ /ZrO ₂ Composite by Fibrous Monolithic Process. Materials Transactions, 2004, 45, 431-434.	1.2	8
243	Hardness behavior of the partially crystallized amorphous Al86Ni9Mm5 alloys. Materials Science & Engineering A: Structural Materials: Properties, Microstructure and Processing, 2003, 363, 81-85.	5.6	24
244	Microstructural Characterization of a Hot Pressed Si ₃ N ₄ -TiN Composite Studied by TEM. Materials Transactions, 2003, 44, 1081-1086.	1.2	2
245	Fabrication of Continuously Porous Alumina Body by Fibrous Monolithic and Sintering Process. Materials Transactions, 2003, 44, 1851-1856.	1.2	12
246	Microstructures and Fracture Characteristic of Si ₃ N ₄ -O’SiAlON Composites using Waste-Si-Sludge. Materials Transactions, 2002, 43, 19-23.	1.2	12
247	Microstructural characterization of electroconductive Si3N4–TiN composites. Materials Letters, 2001, 47, 71-76.	2.6	37
248	Microstructure of rapidly solidified Al–20Si alloy powders. Materials Science & Engineering A: Structural Materials: Properties, Microstructure and Processing, 2001, 304-306, 617-620.	5.6	30
249	Microstructural Characterization of GPSed-RBSN and GPSed-Si ₃ N ₄ Ceramics. Materials Transactions, JIM, 2000, 41, 312-316.	0.9	19
250	Title is missing!. Journal of Materials Science, 1998, 33, 313-318.	3.7	1
251	Stress-Induced Phase Transformation of ZrO2 in ZrO2 (3mol%Y2O3)-25vol%Al2O3 Composite Studied by Transmission Electron Microscopy. Scripta Materialia, 1998, 38, 1101-1107.	5.2	25
252	Nitridation Mechanism of Si Compacts Studied by Transmission Electron Microscopy. Materials Transactions, JIM, 1996, 37, 1547-1553.	0.9	17

#	Article	IF	CITATIONS
253	Microstructure and fracture characteristic of Si3N4î—,ZrO2(MgO) ceramic composite studied by transmission electron microscopy. Scripta Metallurgica Et Materialia, 1995, 32, 1073-1077.	1.0	15
254	Microstructure and fracture behavior of SiC-platelet-reinforced Si3N4 matrix composites. Materials Science & Engineering A: Structural Materials: Properties, Microstructure and Processing, 1994, 177, 151-160.	5.6	10
255	Micro-Indentation Fracture Behavior of Al ₂ O ₃ -24 vol%ZrO ₂ (Y ₂ O ₃) Composites Studied by Transmission Electron Microscopy. Materials Transactions, JIM, 1993, 34, 682-688.	0.9	19
256	Microstructure and Micro-Indentation Fracture of SiC-Whisker-Reinforced Si ₃ N ₄ Composite Studied by High-Resolution Electron Microscopy. Materials Transactions, JIM, 1993, 34, 930-936.	0.9	8